The method of standard porosimetry 2. Investigation of the formation of porous structures

Yu.M. Volfkovich and V.S. Bagotzky
A.N. Frumkin Institute of Electrochemistry, 117071 Moscow (Russian Federation)

(Received February 24, 1993; in revised form September 23, 1993; accepted September 25, 1993)

Abstract

The results obtained by applying the method of standard porosimetry for investigation of different processes in batteries and other electrochemical devices are discussed. The following processes were investigated: swelling and ion exchange of polymeric materials (membranes, conducting polymers); pressing of powdered materials (PVC, Raney silver); the influence of pore-forming agents; chemical and electrochemical sintering of platinum catalysts; deposition of solid products in the pore volume of the cathode during reduction of $SOCl_2$ in lithium batteries; structural changes during formation and cycling of lead and silver oxide electrodes, etc.

Introduction

The laws of formation of porous structures with given properties or of modifications of the porous structure resulting from external influences or from technological processes have not been studied in detail as yet. One of the reasons for this is connected with the fact that the most widespread porosimetric method — the mercury porosimetry (MMP) — is a destructive method and does not give the possibility of repeated measurements on one and the same sample. The method of standard porosimetry (MSP) which was described in ref. 1 is free from this drawback.

This paper describes the results of MSP measurements during formation processes of porous structures.

Nondestructive measurements of structural changes

When investigating changes of the porous structure under the influence of different physical or chemical processes, the possibility of repeated measurements on one and the same sample excludes the influence of a scattering of the initial structural parameters of different samples. This can be illustrated by the results of measurements on the negative electrode of lead/acid batteries [2]. At different stages of their functioning the storage cells were disassembled, one of the negative electrodes was washed, dried and mounted in a special device for porosimetric measurements. After the measurements the electrode was again assembled in the storage cell for further cycling. In Fig. 1 porograms for three electrodes after a starter discharge at −20 °C are shown. The manufacturing process for all three electrodes was the same. In Fig. 2 porograms for

SSDI 0378-7753(93)01876-J

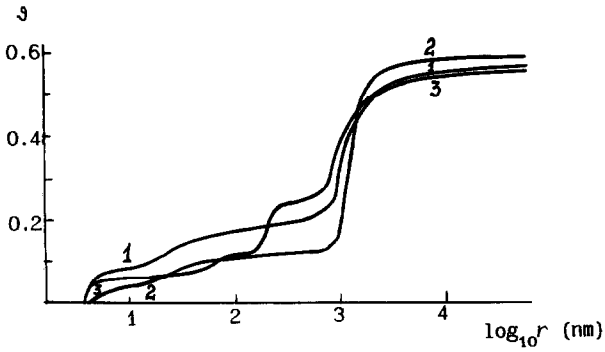

Fig. 1. Integral porograms for three lead electrodes after starter discharge at −20 °C [2].

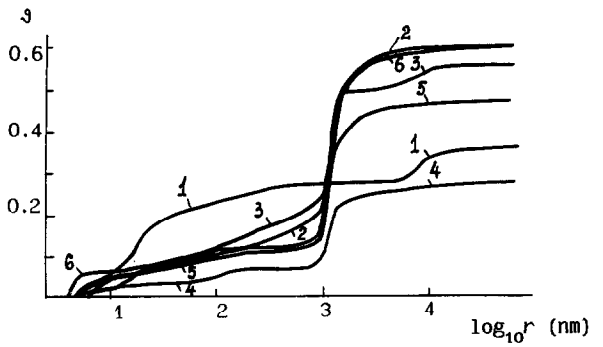

Fig. 2. Integral porograms for a lead electrode after different stages of manufacturing and cycling: (1) pasting; (2) formation; (3) charging; (4) discharge at low current density; (5) starter discharge at +20 °C, and (6) −20 °C [2].

one of them after different treatments are shown. It can be seen that the technological scattering of the structure is comparable with changes of the structure under the influence of some of these processes. Thus, repeated measurements on one and the same sample substantially increases the accuracy and sensitivity of the measurements.

Swelling of porous materials

When a porous material with an insufficiently rigid structure is soaked with a wetting liquid a volume increase (swelling) under the influence of the liquid's capillary pressure p_k is possible. If such a material is used in a liquid medium it is important to know its porous structure just in this medium. The process of swelling depends on the nature of the liquid. In absence of a specific interaction between the porous material and the liquid the capillary pressure is proportional to the surface tension σ of the liquid.

The structure of chrysothyl asbestos widely used as separator in different electrochemical devices (electrolyzers, fuel cells, etc.) was studied. As working liquids octane ($\sigma = 21.7$ mJ/m^2), water ($\sigma = 72.5$ mJ/m^2) and a solution of 7 M KOH ($\sigma = 92$ mJ/m^2 [3]) were used. For alkaline solutions the method described in ref. 4

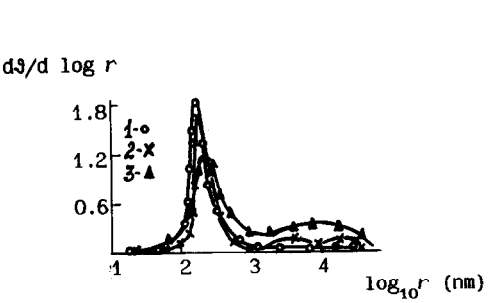

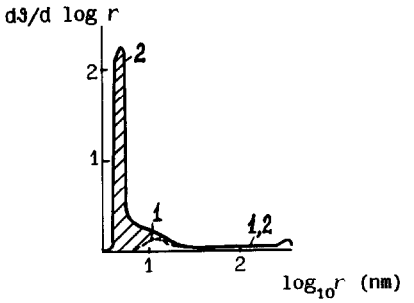

Fig. 3. Differential porograms for asbestos measured with different working liquids: (1) octane; (2) water, and (3) solution of 7 M KOH.

Fig. 4. Differential porograms for the ion-exchange membrane MA-100 measured by means of evaporation of (1) octane and (2) water.

cannot be used since during water evaporation or condensation the solution concentration changes. A modified method was developed in which the amount of liquid in the porous bodies is changed by capillary soaking or drying*. In the first case the dried test sample is contacted with several standard samples filled with different amounts of liquid. In the second case the completely soaked test sample is contacted with dried standard samples. In Fig. 3 differential porograms measured by this method are shown. In octane (curve 1) there is practically no swelling of the asbestos and the porogram is characteristic for its native porous structure. In water (curve 2) swelling is due to an increase of the volume of pores with radii in the range 10^3 to 4.5×10^4 nm. In the alkaline solution (curve 3) there is a further volume increase in the range of the largest pores.

In the case of ion-exchange membranes (solid polymer electrolytes) a different kind of swelling can be observed. From Fig. 4 it can be seen that for the anion-exchange membrane MA-100 in water the pore volume increases almost an order of magnitude mainly as the result of formation of smaller pores (< 10 nm) than in the dry membrane. The same is true for the swelling in water of conducting polymers of the type of polyaniline and poly(*p*-phenylene).

The influence of preliminary soaking and evaporation

Memory effects

When investigating the porous structure of polyaniline in the form of emeraldine chloride or sulfate a peculiar 'memory' effect can be observed which manifests itself in a well-pronounced shape change of the porograms during successive measurements with water as working liquid (Fig. 5) [5]. As a result of pore-volume decrease in the range of micropores the specific surface of the sample decreases substantially. A similar behaviour was observed for the system poly(*p*-phenylene)–acetonitrile [6]. This phenomenon can be tentatively attributed to loosening and subsequent shrinkage of the labile porous structure of these materials during successive soaking and vacuum drying.

*The participation of V.E. Sosenkin, T.N. Toroptseva and N.A. Fedorova in these measurements is acknowledged.

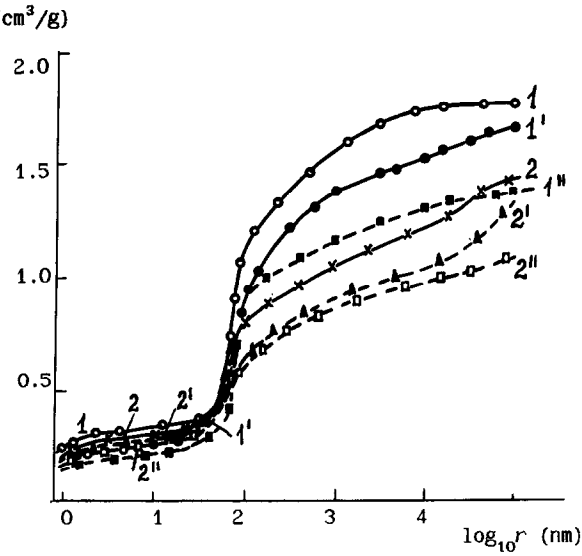

Fig. 5. Integral porograms for (1, 1', 1") emeraldine chloride and (2, 2', ") emeraldine sulfate: (1, 2) first measurement; (1', 2') second measurement, and (1", 2") third measurement [5].

This effect is of great practical significance as the value of the specific surface influences the electrochemical properties of conducting polymers [7].

The influence of ion exchange

Figure 6 shows porograms for the ion-exchange membrane MA-41 (a copolymer of styrene and divinylbenzene with $(NR_3OH)^+$ groups) in the initial sulfate form (curve 1) and after ion exchange in dodecyl ether of sulfoacetic acid (curve 2), in sodium dodecyl sulfate (curve 3) and in sodium decyl sulfate (curve 4) [8]. It can be seen that the porous structure depends upon the nature of the counter ion and that the pore volume significantly decreases upon transition from inorganic to organic anions.

A similar, but even more pronounced behaviour, can be observed for polyaniline in the form of emeraldine salts [9]. In Fig. 7 integral porograms measured with water for chemically synthesized emeraldine chloride (curve 1), and of this salt after ion exchange in sulfuric acid (curve 2) and fluoroacetic acid (curve 3) are shown. It can be seen that the porosity of the chloride form is substantially higher than that of the sulfate form. For the fluoroacetic form in water there is practically no hydrophilic porosity, i.e., this form becomes hydrophobic.

The influence of pressure on the porous structure

Porous materials are often manufactured by pressing of powders. MSP (unlike MMP) gives the possibility to investigate the structure of porous and dispersed materials at fixed values of pressure.

In Fig. 8 porograms for a fixed amount of Raney silver (used as catalyst for oxygen electrodes) measured during a stepwise pressure increase are shown. While

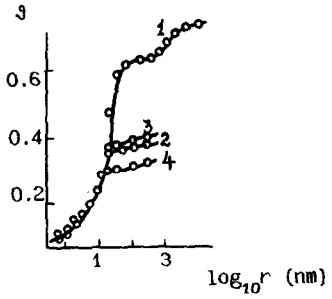

Fig. 6. Integral porogram for the membrane MA-41 stored in different solutions: (1) sodium sulfate; (2) dodecyl ether of sulfoacetic acid; (3) sodium dodecyl sulfate, and (4) sodium decyl sulfate [8].

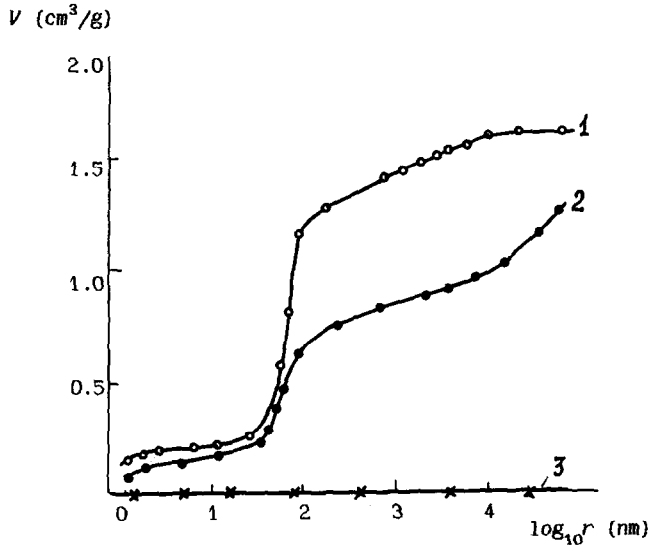

Fig. 7. Integral porograms for salts of emeraldine with the anions: (1) Cl^-; (2) HSO_4^-, and (3) CF_3COO^- [9].

increasing the pressure from 0.05 to 5 MPa, first the volume of the largest pores diminishes, and then the volume of smaller pores in the range from 2×10^4 to 3×10^2 nm. These pores are located between individual particles of the silver catalyst. The structure inside the particles with pores of lower radii (the primary structure) is not altered at the given pressures. However, when increasing the pressure to 10 MPa and higher, a second stage of compressing is reached connected with a destruction of the individual particles. In this case the border between the primary and the secondary structures corresponds to pore radii of about 3×10^2 nm. Thus, MSP gives the possibility to investigate separately the porous structure of individual primary particles and the secondary structure of agglomerates of particles.

A behaviour analogous to Fig. 8 was also observed for other powder samples, e.g., for PVC [10].

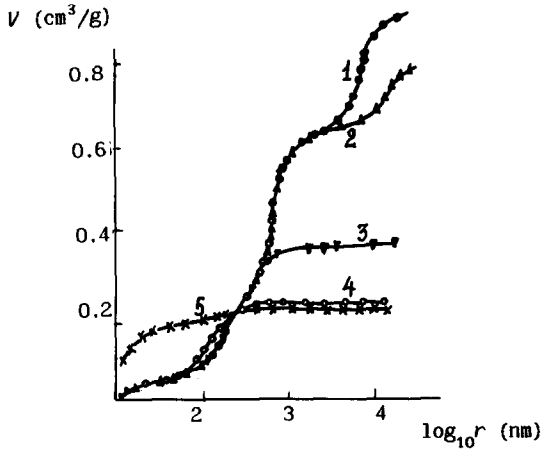

Fig. 8. Integral porograms for pressed Raney silver powder; pressure (MPa): (1) 0.05; (2) 0.2; (3) 5; (4) 10, and (5) 15.

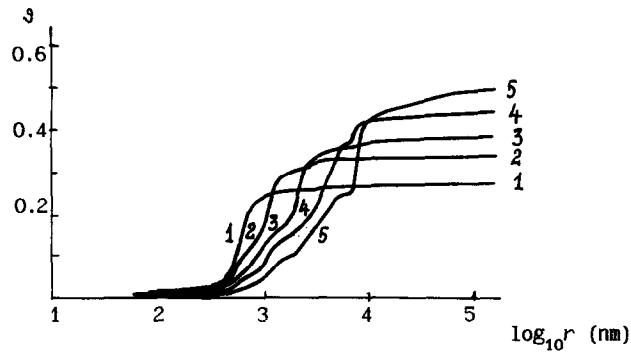

Fig. 9. Integral porograms of titanium electrodes prepared with different concentrations (wt.%) of a pore-forming agent: (1) 0 wt.%; (2) 5 wt.%; (3) 10 wt.%; (4) 15 wt.%, and (5) 20 wt.% [11].

The influence of pore-forming agents

When manufacturing porous products by pressing powders special additives are often used for increasing the amount of coarse pores or for the formation of bidisperse structures.

The influence of pore-forming agents was studied with porous titanium electrodes [11]. These were prepared by pressing powders of titanium and NH_4HCO_3 (45 μm) at 4.5 MPa and subsequent removal of the pore-forming additive at 100 °C. In Fig. 9 the porograms measured with decane for different concentrations (wt.%, c_p) of the pore-forming agent are shown. It can be seen that the electrode has a double porosity. The primary structure with pore sizes below 1 μm is formed between titanium particles and the secondary structure with greater pore sizes by the pore-forming agent. An increase of its amount by 1% leads to an increase of the pore volume by about 1.1%.

These results were obtained by using MSP with evaporation of the working liquid. Therefore they reflect the radii of the blocking pores or 'necks' r_b between trapped pores formed by the additive [1]. The steep rising sections of the porograms correspond to the highest values of r_b. When c_p increased from 5 to 20% the value of r_b increased from 1.3 to 8 μm though the particle size of the pore-forming agent did not change.

The structure of dispersed platinum

During measurements on samples of dispersed platinum, e.g., platinized platinum, many micropores with radii less than 1 nm were found (Fig. 10, curve 1). For platinized platinum these micropores account for more than half of the total pore volume; the radii of most of the remaining pores do not exceed 3 nm. This circumstance is very important since the size of such micropores is comparable with the thickness of the electrical double layer, and also with the size of many molecules and ions, especially organic. Both these factors influence adsorption and kinetic properties of the deposits, particularly their intrinsic catalytic activity [12–15].

The electrochemical sintering of dispersed platinum during polarization for several hours at 0.3 V (RHE) in 0.5 M H_2SO_4 was investigated for electrodes prepared by platinum deposition on a platinum gauze or by pressing platinum black powder at 150 MPa [16]. Figure 10 shows that for the first sample (curve 1) the mean pore size increased from 20 to 40 nm, the specific surface decreased from 28.6 to 17 m^2/g and the overall porosity decreased more than twofold. For the second sample (curve 2) the porosity did not change and the mean pore size of the primary pores increased from 10 to 16 nm, and that of the secondary pores from 20 to 55 nm. The specific surface decreased from 13.8 to 6.5 m^2/g. These results show that electrodes prepared from pressed platinum black, unlike electrodes from platinized platinum, have a rigid structure which prevents shrinkage during polarization.

Deposition of solids in a porous body

In ref. 17 the changes in the structure of a carbon black electrode during thionyl chloride reduction and deposition in the pores of the reaction product LiCl were

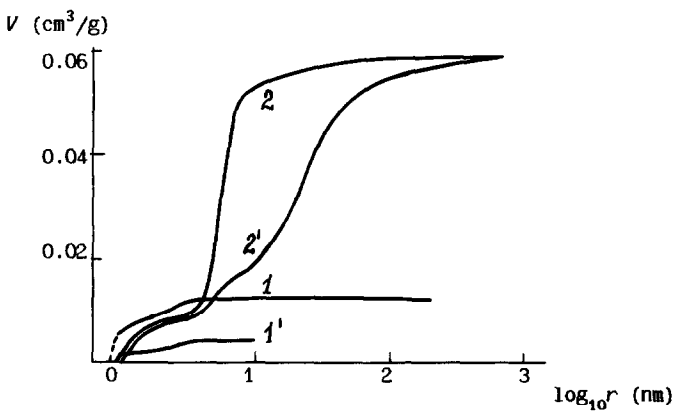

Fig. 10. Integral porograms for (1, 1') platinized platinum and for (2, 2') platinum black (1, 2) before and (1', 2') after electrochemical sintering [16].

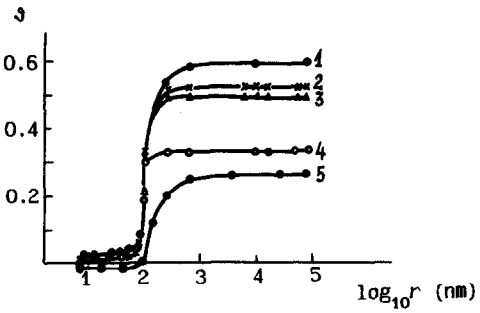

Fig. 11. Integral porograms of a carbon black electrode during thionyl chloride reduction, measured (1) before and after discharge at current density 5 mA/cm^2 to DOD: (2) 13%; (3) 30%; (4) 100%, and (5) porogram of the deposit [17].

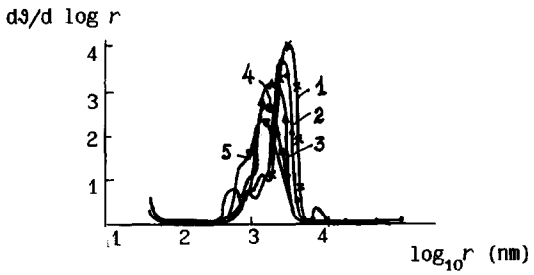

Fig. 12. Differential porograms of a porous titanium electrode (1) before and after platinizing during: (2) 1 min; (3) 3 min; (4) 20 min, and (5) 30 min [11].

investigated. In Fig. 11 porograms are shown which were measured during discharge at a current density of 5 mA/cm^2 up to different values of DOD. It can be seen that the formation of the deposit leads to a significant decrease of the larger pores. At the same time a slight increase of the volume of very small pores can be observed which is due to the filling of large pores with LiCl crystals. The porosity of the filled pores (which is represented by curve 5 and can be calculated by subtraction of curve 4 from curve 1) is only 3.4%. This dense deposit leads to an increase of the thickness of the electrode.

For electrolytic metal deposition on a porous substrate, a different behaviour is observed as in this case the deposit is formed not in the volume of the solution in the pores but directly on the pore surface. In Fig. 12 porograms of an electrolytically platinized porous titanium electrode are shown [11]. It can be seen that platinizing leads to a shift of the maximum of the distribution curve towards smaller pore sizes and to a gradual lowering of the radii of practically all pores. During platinizing there is a gradual increase of small pores with radii less than 100 nm inside the platinum deposit.

Solid-state reactions in storage cells

The investigation of structural changes of battery electrodes during discharge and during cycling is of great importance for a better understanding of their properties.

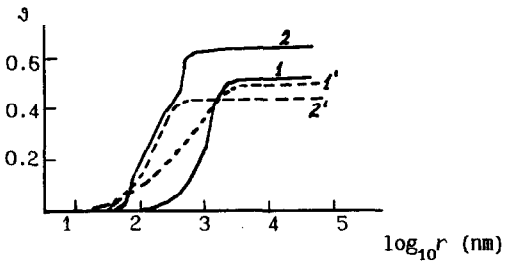

Fig. 13. Integral porograms of silver electrodes prepared from (1, 1') standard silver powder and (2, 2') reduced AgCl measured (1, 2) before and (2, 2') after formation [18].

As most of the metals used in such electrodes (lead, cadmium, silver, etc.) are easily amalgamated MMP cannot be used for this purpose.

From the porogram for the negative electrode of the lead/acid cell (Fig. 2) it can be seen that the freshly pasted electrode (curve 1) has a double porosity with a great amount of pores of radii between 7 and 300 nm and a smaller amount of pores between 6 and 10 μm. After formation (curve 2), the main amount of pores corresponds to a narrow range between 800 and 3200 nm while the remaining amount is spread over the range between 5 and 800 nm. A significant part of pores in the range of 800 to 3200 nm is maintained for all states-of-charge of the electrode during cycling. Thus, the main effect of the formation process of lead electrodes is the development of pores in this range. It seems that these pores are important for the transport of HSO_4^- ions, particularly at high current densities. The localization of the structural changes in a narrow range of pore sizes is probably beneficial for the reversibility of the structure during cycling and thus for enhancing the cycle life of the storage cell. The great difference between the overall porosities in the charged and discharged states is due to the high ratio of the densities of metallic lead and lead sulfate (1.8:1).

For the silver electrode in silver–zinc batteries, the main parameter is the efficiency of silver utilization (transformation into AgO) during charging. This efficiency increases with decreasing charging-current density and with increasing discharge-current density. These observations can be compared with structural changes. In Fig. 13 porograms are shown for electrodes manufactured from commonly used silver powder (1, 1') and from fine powder prepared by reduction of AgCl (2, 2') both before formation (1, 2) and after formation (1', 2') during two cycles [18]. For the initial electrodes 1 and 2 the values of the specific surface calculated from the porograms were 0.2 and 2.19 m^2/g and the efficiencies 47% and 77%, respectively. After formation the corresponding values were 0.87 and 1.14 m^2/g for the specific surface and 72 and 73% for the efficiency. Thus, after formation, the properties of the electrodes and their structure are levelled off. Recrystallization during cycling leads to a loss of the 'memory' of the initial structure. The increase of efficiency with increasing discharge-current density can be attributed to an increase of the specific surface of silver.

MSP was also applied to several other materials and processes, e.g., the polymerization of vinyl chloride to poly(vinyl chloride) [10], the sintering of porous titanium electrodes [11], the storage of electrodes of the silver–zinc storage cell, the preparation of an ion-exchange membrane from the corresponding ion-exchange resins, etc.

References

1 Yu.M. Volfkovich and V.S. Bagotzky, *J. Power Sources, 48* (1993) 327–338.
2 E.S. Livshits, E.G. Yampolskaya and Yu.M. Volfkovich, *Elektrokhimiya, 19* (1983) 1275–1278.
3 P.M. Dunlap and S.R. Faris, *Nature, 196* (1962) 1312–1313.
4 Yu.M. Volfkovich, V.S. Bagotzky, V.E. Sosenkin and E.I. Shkolnikov, *Elektrokhimiya, 16* (1980) 1620–1652.
5 Yu.M. Volfkovich, T.K. Zolotova, M.D. Levy and Ya.A. Letuchii, *Adv. Mater., 4* (1993) 274–276.
6 Yu.M. Volfkovich, M.D. Levi, T.K. Zolotova and E.Yu. Pisarevskaya, *Polym. Comm., 39* (1993) 2443–2446.
7 Yu.M. Volfkovich, T.K. Zolotova, S.L. Bobe and A.V. Shlepakov, *Elektrokhimiya, 29* (1993) 897–903.
8 N.A. Kononenko, N.P. Berezina, Yu.M. Volfkovich, E.I. Shkolnikov and I.A. Blinov, *Zh. Prikl. Khimii, 58* (1985) 2199–2203.
9 T.K. Zolotova, A.V. Shlepakov and Yu.M. Volfkovich, *Elektrokhimiya, 29* (1993) 630–635.
10 V.T. Marinin, D.N. Bort, B.S. Zavyalova and Yu.M. Volfkovich, *Vysokomol. Soedin., Ser. A, 22* (1980) 1736–1741.
11 N.V. Kuleshov, Yu.M. Volfkovich, E.L. Filippov and E.I. Shkolnikov, *Elektrokhimiya, 14* (1978) 1887.
12 V.F. Stenin and B.I. Podlovchenko, *Vestn. Mosk. Univ., Ser. Khim., 4* (1967) 21–24.
13 O.A. Khasova, Yu.B. Vassilyev and V.S. Bagotzky, *Elektrokhimiya, 6* (1970) 1367–1370.
14 P. Stonehart and J. Lundquist, *Electrochim. Acta, 18* (1973) 907–911.
15 B.I. Podlovchenko, T.D. Gladysheva, O.V. Vyaznikovtseva and Yu.M. Volfkovich, *Elektrokhimiya, 19* (1983) 424–428.
16 T.D. Gladysheva, E.I. Shkolnikov, Yu.M. Volfkovich and B.I. Podlovchenko, *Elektrokhimiya, 18* (1982) 436–442.
17 V.S. Bagotzky, V.E. Kazarinov, Yu.M. Volfkovich, L.S. Kanevsky and L.A. Beketayeva, *J. Power Sources, 26* (1989) 427–433.
18 V.P. Sirotinskaya, Yu.M. Volfkovich, V.E. Sosenkin and I.E. Yablokova, *Elektrotekhnicheskaya Promyshlennost', Ser. Khim. i. fis. istochnikov toka, 6* (1983) 18–20.